

Article

High-Intensity Ultrasound Pulses Effect on Physicochemical and Antioxidant Properties of Tilapia (*Oreochromis niloticus*) Skin Gelatin

Dulce Alondra Cuevas-Acuña ¹, Joe Luis Arias-Moscoso ², Wilfrido Torres-Arreola ³,
Francisco Cadena-Cadena ³, Ramón Gertrudis Valdez-Melchor ¹, Sarai Chaparro-Hernandez ⁴,
Hisila del Carmen Santacruz-Ortega ⁵ and Saúl Ruiz-Cruz ^{4,*}

¹ Departamento de Ciencias de la Salud, Univerisdad de Sonora, Ciudad Obregón 85040, Mexico; dulce.cuevas@unison.mx (D.A.C.-A.); ramon.valdez@unison.mx (R.G.V.-M.)

² Departamento de Ingenierías, Instituto Tecnológico del Valle del Yaqui, Bácum 85276, Mexico; jarias.moscoso@itvy.edu.mx

³ Departamento de Investigación y Posgrado en Alimentos, Univerisdad de Sonora, Hermosillo 83000, Mexico; wilfrido.torres@unison.mx (W.T.-A.); francisco.cadenac@unison.mx (F.C.-C.)

⁴ Departamento de Biotecnología y Ciencias Alimentarias, Instituto Tecnológico de Sonora, Ciudad Obregón 85000, Mexico; sarahich54@gmail.com

⁵ Departamento de Investigación en Polímeros y Materiales, Univerisdad de Sonora, Hermosillo 83000, Mexico; hisila@polimeros.uson.mx

* Correspondence: saul.ruiz@itson.edu.mx; Tel.: +55-644-410-9000

Received: 31 December 2019; Accepted: 29 January 2020; Published: 3 February 2020



Abstract: Ultrasonic pulses are considered green technology for the improvement of the functional properties of proteins. In this study, four high-intensity ultrasound pulse treatments (ultrasound-pulsed gelatin (UPG)-42, UPG-52, UPG-71, UPG-84, and non-pulsed control gelatin (CG)) were applied to tilapia (*Oreochromis niloticus*) skin gelatin in order to study their effect on its physicochemical and antioxidant properties; a non-treated gelatin was used as a control. UPGs showed a significant increase in soluble protein and surface hydrophobicity compared to the control gelatin, and no significant difference was found in the electrophoretic profiles. The effects on the secondary structure were studied by circular dichroism and infrared spectra, and these showed that the random coil conformation was the main component in all treatments and the ultrasonic treatments only affected the α -helix and β -sheet proportion. Finally, the ABTS ((2,2'-azino-bis-(3-ethylbenzothiazoline-6-sulfonic acid)) and FRAP (ferric reducing ability) assays demonstrated that ultrasound treatments could improve the antioxidant activity of gelatins as free radical scavengers and electron donors. These results suggest that high-intensity ultrasound pulse technology is useful to improve fish gelatin antioxidant properties, which could be associated with secondary structure disruption.

Keywords: high-intensity ultrasound pulses; gelatin; antioxidant; unfolding

1. Introduction

In recent years, ultrasonic pulses have been used as an environmentally-friendly technology to improve the functional properties of vegetable and animal proteins by altering their hydrogen bonds and hydrophobic interactions, as well as by disrupting their molecular conformation through cavitation, heating, dynamic agitation and shear stress [1]. Additionally, this technology has been used in green chemistry as a tool for the extraction of functional compounds with an improved yield, short time, low cost, and less solvent [2].

Ultrasound consists of an acoustic wave with a frequency greater than 20 kHz that is undetectable to the human ear and which spreads in a medium; the application of ultrasound can be classified into two major groups: low-intensity and high-intensity ultrasound. High-intensity ultrasound (HIU) consists of low frequency (20–100 kHz), and a high power ($>1 \text{ W/cm}^2$) is preferred since it provokes more substantial effects on a substrate [3]. The ultrasound mechanism of action is based on the passage of waves that create regions of high and low pressure; this variation in acoustic pressure is directly proportional to the amount of energy applied to the system [3]. The propagation of high-intensity ultrasound in a liquid induces a series of compressions and decompressions, causing molecular displacement by disrupting dipole–dipole, hydrogen bonding, and other weaker interactions.

The conventional process of extracting gelatin from tilapia skin consists of the thermal denaturation of the collagen that, in its native form, is found as a triple helix of polypeptide chains. The acid and alkali chemical treatments remove the soluble proteins. Finally, the heat treatment interrupts intramolecular interactions, thus causing the triple helix to open and exposing the hidden hydrophobic groups towards the inside of the helix. The high-intensity ultrasonic treatments that are applied to the system energy disrupt weak intramolecular interactions, and this causes changes in the conformation of the protein by the splitting of the polypeptide chains.

High-intensity ultrasound pulses have been tested for collagen extraction at an industrial level, and favorable results were obtained because it was possible to minimize the extraction time (from 24 to 3 h) and acid concentration (from 0.5 to 0.05 M) while obtaining twice the yield compared to the conventional method. The industrial system for this process consists of a collagen separation device (where ultrasound is generated and collagen is separated from the sample), a cooling unit, sample supply, a discharge pipe, and circulation pump [2].

Among the most relevant findings about the effect of HIU on proteins is the increase in the solubility of protein suspensions, which is considered to be one of the main requirements during the improvement of the other functional and biological properties of proteins; however, not using proper power and time conditions can lead to the denaturation of proteins due to the overexposure of hydrophobic residues [1,4,5].

Other studies have found that ultrasonic treatments reduce the size of proteins [6], and cavitation can promote the deployment of proteins, causing the exposure of hydrophobic and electrostatic regions; therefore, the capacity of the proteins to interact with oil in an emulsion can be improved [7]. Additionally, according to some findings, pulsed ultrasound increases sulfhydryl groups and hydrophobicity due to the unfolding of the secondary structure of the protein [8,9]. HIU also affects the secondary and tertiary structure of quinoa proteins, changes which result in an increase in solubility and particle size, improving the protein's potential in the food industry [10].

In addition to their functional properties, proteins have also been used as a source of molecules with biological activity, with antioxidant activity being one of the most studied [11]. Ultrasound has also been used as a pretreatment during protein hydrolysis to improve the bioactivities of hydrolysates [12]. In regard to tilapia skin gelatin, the antioxidant activity refers to peptides or low molecular weight polypeptide chains [11–14]. On the other hand, tilapia fishing generates a considerable amount of by-products, such as skin, scales, heads, and bones, which are discarded and generate pollution in the environment [15]; if these by-products are given an alternative use, it would be possible to reduce pollution and to favor the integral use of this species—hence the intention of using them in the present investigation.

In summary, HIU directly affects the physicochemical properties of proteins through conformational changes that are conditioned to the intensity and timing of the ultrasonic pulses, as well as the native state of the protein. HIU pulses can be considered an important technique for the improvement of protein properties that are extracted from fisheries waste because information on the effect of ultrasound on the structure and antioxidant properties of marine proteins is limited. Therefore, this work aimed to study the impact of HIU pulses on the physicochemical and antioxidant

properties of gelatin, one of the most important regional fishery products, to improve the utilization of tilapia waste through green technology.

2. Materials and Methods

2.1. Raw Materials and Reagents

Skins of Nile tilapia (*Oreochromis niloticus*) was obtained from the Oviachic Dam in Cajeme, Mexico, and then they were transported frozen and in ice to the facilities of CIIBAA (Centro de Investigación e Innovación Biotecnológica, Agropecuaria y Ambiental), where they were peeled, washed and stored at $-30\text{ }^{\circ}\text{C}$ until processing. ABTS (2,2'-azino-bis-(3-ethylbenzothiazoline-6-sulfonic acid)), iron chloride, 2,4,6-tri(2-pyridyl)-s-triazine, Trolox (6-hydroxy-2,5,7,8-tetramethylchroman-2-carboxylic acid), and BSA (bovine serum albumin) were obtained from Sigma-Aldrich (Mexico). All other chemicals that were used in this study were of analytical grade and commercially available.

2.2. Gelatin Extraction

Gelatin was extracted, as reported by [16]. The skin pretreatment consisted of soaking the skins in alkali (0.77 N NaOH, 1:5 *w/v* for 1 h) and then rinsing until the pH dropped to 7; this was repeated with an acid solution (0.59 N HCl 1:5 *w/v* for 1 h), after which the skins were rinsed and pressed again. The skins were placed into glass beakers containing distilled water (1:3 *w/v*), and then they were covered with aluminum foil. The gelatin extraction consisted of using a water bath at $66\text{ }^{\circ}\text{C}$ for 6 h. Then, the gelatin solution was filtered by using a cheesecloth, and the solution was lyophilized in a freeze dryer (Freeze zone 4.5, Labconco; Argentina) for 5 days.

2.3. High-Intensity Ultrasound Pulses Treatments

Samples of fifty milliliters of gelatin solutions (10 mg/mL) at pH 7.0 in 100 mL beakers that were immersed in an ice-water bath were subjected to HIU pulses that consisted of two amplitudes (50% and 100%) and two time periods (1 and 2 min) with a pulse duration of on-time 10 s and off-time 5 s; this was performed by using an ultrasonic processor (VCX750, Vibra cell, Sonics; USA) with a 13-mm, high-grade titanium alloy probe and a net power of 750 W at a frequency of 20 kHz. HIU pulse treatments were carried out in triplicate. Temperature and pH readings were taken for each sample at the beginning and end of the treatments with a pH meter (Hanna pH/mV/ $^{\circ}\text{C}$ meter HI2211, USA). The acoustic power of the treatments was calculated as reported previously [7]. Ultrasound-pulsed gelatins (UPG) and a non-pulsed gelatin (CG) solutions were frozen at $-80\text{ }^{\circ}\text{C}$ and later lyophilized in a freeze dryer (Freeze zone 4.5, Labconco; Argentina) for 24 h. Lyophilized gelatin powders were subjected to characterization analysis, which was performed at $25\text{ }^{\circ}\text{C}$.

2.4. Protein Solubility

The soluble protein was measured with the micro assay protocol of the Bradford method [17]. Gelatins were dissolved in a phosphate buffer (pH 7.4) and centrifuged at $13,000\times g$ for 15 min at room temperature. The supernatants (5 μL) and the dye reagent (250 μL) were added to the well; this blue protein–dye form was detected at 595 nm by using a microplate reader (Thermo Scientific Multiskan Sky; USA). A BSA standard curve was used to calculate the soluble protein in the gelatin solutions. Results are presented as the percentage of the soluble protein in the total gelatin protein. Determinations were carried out by sixfold for each sample.

2.5. Molecular Weight Distribution

The analysis of the gelatin protein fractions was carried out by polyacrylamide–sodium dodecyl sulfate gel electrophoresis (SDS-PAGE) according to the method of Laemmli [18]. The sodium dodecyl sulfate–polyacrylamide gels consisted of 10% acrylamide in the resolving gel and 4% acrylamide in the stacking gel. Samples were mixed with a reducing sample buffer 1:1 (*v/v*) and heated at $95\text{ }^{\circ}\text{C}$ for

5 min, after which 12 μL of these samples were loaded into each lane of the gel. The electrophoresis was performed in a Mini-PROTEAN Tetra slab cell (Bio-Rad Laboratories; USA) at 120 V in a running buffer. Finally, the gels were stained with Coomassie Blue R250, and the excess was removed with a solution of methanol:water:acetic acid 5:4:1 (*v/v/v*) until the bands were visible.

2.6. Surface Hydrophobicity

The protein surface hydrophobicity of the gelatins was determined by using 1-anilino-8-naphthalenesulfonate (ANS) as a hydrophobic probe [19]. The gelatin solutions (1 mg mL^{-1}) were prepared in a 0.1 M phosphate buffer (pH 7.0) and serially diluted in the same buffer; 2 mL of each dilution was added to 10 μL of a 10 mM 1-anilino-8-naphthalene sulfonic acid (ANS) solution. The fluorescence intensity was registered at 485 nm (emission) and 375 nm (excitation) by using a fluorescence spectrophotometer (Agilent Technologies, Cary Eclipse; USA). Five replicates were carried out for each sample. The surface hydrophobicity is reported as the slope of the fluorescence intensity vs. the protein concentration plot.

2.7. Circular Dichroism

The circular dichroism (CD) spectra of the gelatins were obtained by utilizing a CD spectropolarimeter (J-815; JASCO, Japan) with the Peltier accessory (PFD-425S/15; JASCO). Samples were prepared at a protein concentration of 0.125 mg mL^{-1} in a phosphate buffer. Scanning wavelengths ranging from 190 to 240 nm were registered. The analysis was carried out from 5 to 90 °C. The secondary-structure components' percentage of the gelatins was calculated with the DichroWeb website (<http://dichroweb.cryst.bbk.ac.uk/html.shtml>); all data are the average of three determinations.

2.8. Fourier-Transform Infrared Spectra

FTIR spectra provide information about the secondary structure content of proteins. Fourier-transform infrared spectra were obtained from 1 mg of the lyophilized gelatins. Readings were conducted at 25 °C by using an infrared spectrometer (Frontier FTIR; Perkin Elmer; USA) with an attenuated total reflections (ATR) accessory at a scanning interval ranging from 500 to 4000 cm^{-1} . Results are expressed in graphs of absorbance versus wavenumber (cm^{-1}).

2.9. ABTS Radical Cation Scavenger

The gelatin ABTS radical scavenging capacity was assessed by using a modified version of the method of Re [20]. A stock solution of the ABTS radical was prepared by mixing 5.0 mL of a 7 mM ABTS solution with 88 μL of 139 mM potassium persulfate that was kept in the dark at room temperature for 18 h. An aliquot (0.5 mL) of the stock solution was diluted with a phosphate buffer (50 mM, pH 7.4) to prepare the working solution of the ABTS radical with an absorbance of 0.70 ± 0.02 at 734 nm. The gelatin solutions (5% *p/v*) were prepared in the same buffer, and the buffer was used as a blank. For this analysis, a 20 μL aliquot of the sample was mixed with 280 μL of the ABTS radical working solution, which was incubated for 30 min at room temperature in the dark, and then the absorbance was measured at 734 nm by using a microplate reader (Thermo Scientific Multiskan Sky; USA). A standard curve of Trolox was used to express the results as Trolox equivalents/mg sample (TE/mg). Six replicates were carried out for each sample.

2.10. Ferric Reducing Antioxidant Power

The ferric reducing ability (FRAP) of the gelatins was assessed as described by Benzie [21]. The working solution was prepared by mixing an acetate buffer (300 mM, pH 3.6), a TPTZ (2,4,6-tripyridyl-s-triazine) solution (10 mM), and an $\text{FeCl}_3 \cdot 6\text{H}_2\text{O}$ solution (20 mM) in a 10:1:1 ratio, respectively. The gelatin solutions (5% *p/v*) were prepared in a 50 mM phosphate buffer (pH 7.4).

A 20 μL aliquot of the sample was mixed with 280 μL of the working solution; after 30 min, the absorbance at 595 nm was registered by using a microplate reader (Thermo Scientific Multiskan Sky; USA). A standard curve of Trolox was used to express results as Trolox equivalents/mg sample (TE/mg). Six replicates were carried out for each sample.

2.11. Statistical Analysis

The effect of the ultrasound pulses was determined by ANOVA, followed by Tukey's test at $\alpha = 0.05$ by using the JMP software (Version 5.0.1, SAS Institute. Inc.; USA). Different letters in tables indicate a significant difference.

3. Results and Discussion

3.1. Ultrasound Pulses

Under the conditions of the present study, the acoustic intensity of the treatments with 50% amplitude for 1 and 2 min was 42 and 52 W/cm^2 , respectively, while for treatments with 100% amplitude, the intensity was 71 for 84 W/cm^2 for 1 and 2 min, respectively. Henceforth, the treatments are identified as UPG-42, UPG-52, UPG-71, and UPG-84, respectively, and CG (control gelatin). During the ultrasonication of the gelatins, a maximum increase of 0.8 $^{\circ}\text{C}$ was recorded, ensuring that the conformational changes in the proteins were due to cavitation and not because of a temperature increase. On the other hand, the pH of the UPG decreased by 0.78 units, showing a significant difference concerning the CG. However, although the pH decreased as the intensity of the treatments increased, there were no significant differences between them ($p < 0.05$). The decrease in pH has previously been associated with transitional changes that result in the deprotonation of acidic amino acid residues. This can affect intramolecular interactions and the conformation of protein chains by exposing new residues to the aqueous medium. The decrease in pH for the samples treated with ultrasound has been previously reported for vegetable and animal proteins, including fish gelatin [6].

3.2. Protein Solubility

Protein solubility is used as the primary indicator of functionality and is subjected to the state of denaturation or aggregation. The percentages of soluble proteins of the UPG and the CG are shown in Table 1. Concerning the CG, solubility significantly increased for all gelatins except for UPG-52, and no significant differences were found between the rest of the treatments. The increase in the solubility of proteins has been related to changes in conformation that are caused by cavitation (as mentioned above), by the exposure of more internal hydrophilic residues to the water surface, by the interruption of hydrophobic interactions in insoluble aggregates, and also by changes in the electronic environment of the acid residues related to the effect of pH. This behavior in protein solubility has been previously reported in HIU studies, although it has also been reported that the prolongation of these treatments can generate insoluble aggregates [5,9,10,22].

Table 1. Antioxidant activity, pH, protein solubility, and surface hydrophobicity of tilapia (*Oreochromis niloticus*) skin gelatins that were treated with high-intensity ultrasound pulses.

Treatment	pH	Soluble Protein (%)	Surface Hydrophobicity	ABTS (μM TE/mg gelatin)	FRAP (μM TE/mg gelatin)
Control	7.00 \pm 2.0 ^a	27.6 \pm 8.3 ^b	62.1 \pm 7.7 ^c	539 \pm 73 ^c	112 \pm 32 ^c
UPG-42	6.40 \pm 0.2 ^b	43.6 \pm 1.2 ^a	71.7 \pm 6.5 ^b	301 \pm 88 ^d	244 \pm 50 ^b
UPG-52	6.30 \pm 0.2 ^b	27.4 \pm 3.9 ^b	75.2 \pm 4.9 ^{ab}	209 \pm 28 ^d	293 \pm 15 ^b
UPG-71	6.08 \pm 0.3 ^b	43.7 \pm 1.6 ^a	66.5 \pm 4.0 ^b	698 \pm 65 ^b	385 \pm 143 ^b
UPG-84	6.10 \pm 0.2 ^b	42.0 \pm 2.9 ^a	81.4 \pm 6.3 ^a	1001 \pm 38 ^a	732 \pm 91 ^a

Values are the mean of $n = 6 \pm$ the standard deviation. Different superscripts in each column indicate significant differences between ultrasonic pulsed gelatin ($p < 0.05$).

3.3. Surface Hydrophobicity

Protein surface hydrophobicity is determined by the content of hydrophobic residues on the surface of a molecule and is, therefore, an indicator of protein unfolding. In collagen, these hydrophobic residues are hidden inside the triple helix; however, when the gelatin forms disordered polypeptide chains, it already has a higher hydrophobic surface due to new residues exposed on the surface. In this study, the different treatments of HIU showed a significant increase in surface hydrophobicity of the control without treatment ($p < 0.05$) (Table 1).

In the present study, the highest hydrophobicity values corresponded to the treatments UPG-52 and UPG-84 (treatments for 2 min); this behavior was in agreement with the previous study for HIU for the giant squid protein, with an amplitude of 40% for 90 s, as well as for wheat proteins when using 31 W/cm² for 20 min and scallop proteins when using 3361.64 W/cm² for 1 h [7,8,22]. All of these studies reported the highest surface hydrophobicity for the most intense and extended treatment. The results of this investigation could be attributed to the unfolding of polypeptide chains by the interruption of non-covalent interactions, allowing for an increase in the exposure of hydrophobic gelatin residues.

3.4. Molecular Weight Distribution

Polyacrylamide gel electrophoresis under reducing conditions was used to separate protein fractions by molecular weight. Figure 1 shows the electrophoretic profile of the gelatins. In the CG lane, there are two bands called component β and α ; the first represents a dimer of covalently linked α chains with a molecular weight around 200 kDa, while the second represents polypeptide chains of around 100 kDa that are typical of gelatin. In the case of the lanes with UPGs, we can see the same electrophoretic profile for different treatments, and the differences in band intensities between the ultrasound pulsed gelatins could be related to protein solubility. The absence of new bands of lower molecular weights indicates that none of the treatments resulted in the hydrolysis of polypeptide chains, and, therefore, the primary structure of the control gelatin was preserved. These results are consistent with those previously reported for egg white, bovine, fish gelatin [6], chicken myofibrillar protein [5], and squid mantle protein [7]. It is worth mentioning that the slight increase in the intensity of bands for the UPG-71 and UPG-84 lanes could be attributed to the fact that the intensity of these treatments caused more significant protein aggregation.

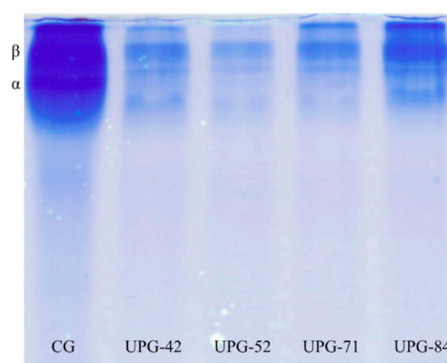


Figure 1. SDS-PAGE profile of tilapia (*Oreochromis niloticus*) skin gelatins that were treated with high intensity ultrasound pulses.

3.5. Circular Dichroism

Circular dichroism was used to study the effect of the HIU treatments on the secondary structure of the gelatins because this technique allows for the calculation of the proportion of each component (α helix, β sheet, and random coil) in gelatins. Figure 2A shows the proportions of components in all gelatins at 25 °C; all gelatins showed a higher proportion of random coils, which was followed

by the α -helix, and finally by the β -sheets in a smaller proportion. This is consistent with changes resulting from the denaturation of collagen (triple helix) to gelatin. The changes in the secondary structure of gelatins were caused by the conformations acquired by the atoms of the backbone of the polypeptide chain induced by cavitation. Previous studies have related the reduction of the α -helix with protein unfolding and the increase of the β -sheet with protein aggregation [12]. Additionally, it can be seen that the HIU treatments generated significant differences in the secondary structure at increasing temperatures from 10 to 90 °C, as shown in Figure 2B–F, where although the random coil was the major secondary structure for all gelatins, UPG-71 and UPG-84 had a substantial change in the β -sheet/ α -helix ratio at around 60 °C.

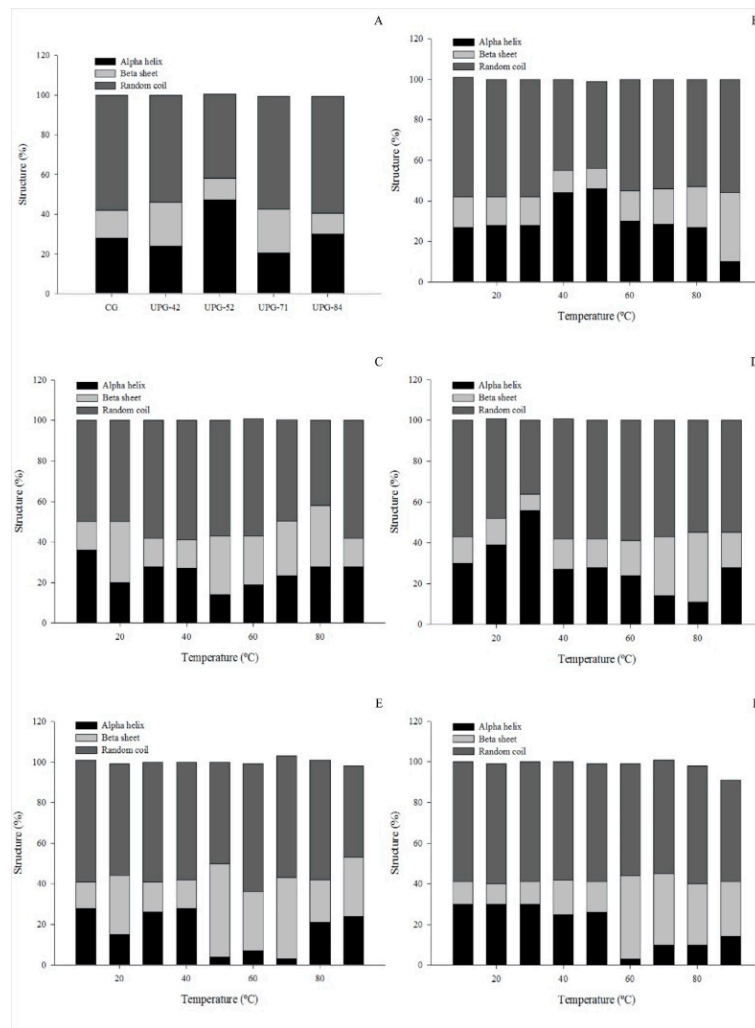


Figure 2. Secondary structure composition of ultrasound pulsed tilapia (*Oreochromis niloticus*) skin gelatin. (A): Secondary structure composition of gelatins at 25 °C. (B–F): Secondary structure composition in a temperature range of 10 to 90 °C of the control gelatin (CG), ultrasound-pulsed gelatin (UPG)-42, UPG-52, UPG-71, and UPG-84, respectively.

For the control gelatin, the most substantial changes occurred at approximately 40 °C, where there was a 37% increase in the α -helix (Figure 2B), while the random coils decreased; this may have been due to the unfolding of the remaining collagen, since the collagen from marine species presented little cross-linking, confirmed by its low thermal denaturation temperature at ~40 °C, corresponding to a poorly cross-linked collagen [23]. Additionally, as the temperature rose, it could be seen that the β -sheet structure began to have a progressive increase until reaching 64% of this structure; as this

happened, and while the random coil remained constant, the α -helix could have been transforming into a β -sheet.

As for UPG-42 (Figure 2C), as the temperature rose, the random coil remained the dominant component; however, the β -sheets began to predominate over the α -helix, reaching their lowest point around the denaturation temperature. For UGP-52 (Figure 2D), there was a 21% increase in the α -helix at around 30 instead of 40 °C [24]. In the case of UPG-71 (Figure 2E), the denaturation temperature was low, around 37 °C, which implied drastic changes in the β -sheet and the α -helix, resulting in a loss of 87.5% of the α -helix and an increase in the β -sheet. Finally, in the case of UPG-84 (Figure 2F), the denaturation took place at around 40 °C. However, changes in the secondary structures began to occur from 30 °C in the α -helix, even reaching temperatures of 60 °C, at which almost all of the α structures were lost.

These α -helix decreases and β -sheet increases are consistent with those that have been reported for scallops [9], but they contrast with those that have been reported for lactic proteins [25]. These results indicate that the high-intensity ultrasonic pulses that were used in this work affect even the secondary structure and denaturation temperature of gelatins due to the alteration in interactions between polypeptide chains.

3.6. Fourier-Transform Infrared Spectra

The IR spectra for the proteins included the characteristic bands of amides I, II, A, and B (Figure 3). The bands of amide A ($\sim 3300\text{ cm}^{-1}$) and amide B ($\sim 3000\text{ cm}^{-1}$) are associated with vibrations of NH stretching, the presence of hydrogen bonds, and the asymmetric stretching of CH_2 [26]. The amide I band ($\sim 1600\text{ cm}^{-1}$) represents the stretching vibrations of the carbonyl bond ($\text{C}=\text{O}$) from the amide (peptide bond), the amide II band ($\sim 1500\text{ cm}^{-1}$) is attributed to the bending vibrations of the N-H bond, and the amide III ($\sim 1200\text{--}1300\text{ cm}^{-1}$) complex bands result from a mixture of several coordinate displacements [24]. These bands are essential to determine secondary structures because they are in the backbone of polypeptide chains, and their hydrogen bridge interactions give place to different conformations (α -helix, β -sheet, and random coil).

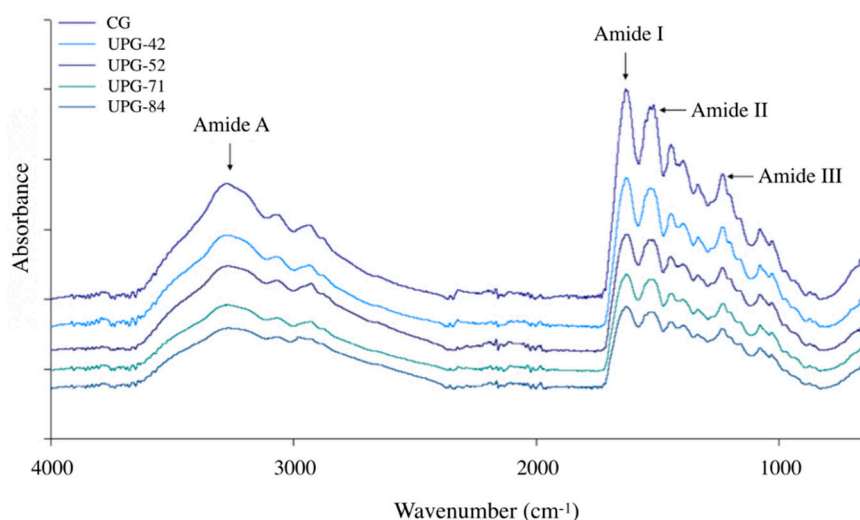


Figure 3. FTIR spectra of tilapia (*Oreochromis niloticus*) skin gelatins that were treated with high intensity ultrasound pulses.

The FTIR spectra of the UPG and the CG are depicted in Figure 3. Similar patterns in FTIR spectra, including amides A ($3269\text{--}3272\text{ cm}^{-1}$), I ($1629\text{--}1632\text{ cm}^{-1}$), II ($1516\text{--}1532\text{ cm}^{-1}$), and III ($1231\text{--}1234\text{ cm}^{-1}$) were observed. As the intensity of the ultrasonic treatment increased, slight displacements ($\sim 3\text{ cm}^{-1}$) were shown towards higher wavenumbers in the case of amides A, I, and III; however, the amide II peak for the UPG (1532 cm^{-1}) showed a significant displacement (16 cm^{-1}) with respect to the CG (1516

cm^{-1}). These higher wavelength shifts with increasing ultrasound intensity have been related to the loss of ordered structures (unfolding) by an increase in the interruption of intermolecular interactions, which has been associated with more severe extraction conditions for gelatin [27].

As mentioned before, the amide I and II peaks are the leading indicators of changes in the secondary structure, and it is assumed that the displacement of these bands is a product of the changes and disorder in the conformations of the secondary structures when increasing the intensity of the ultrasonic pulses [10,25,27]. These results may be related to the results in the previous section, where it was shown that the different treatments caused significant changes in the proportions of the α -helix and the β -sheet in the UPG.

3.7. ABTS Radical Cation Scavenger

The results of antioxidant activity are shown in Table 1. The ABTS assay showed significant differences between the UPG and the CG. For the CG (539 $\mu\text{M TE}$), the less intense treatments UPG-42 and UPG-52 showed significant decreases in activity (301 and 209 $\mu\text{M TE}$, respectively), while the higher intensity treatments UPG-71 and UPG-84 showed significant increases (698 and 1001 $\mu\text{M TE}$, respectively; $p < 0.05$). Therefore, the conformational changes that were generated by the treatment with 100% amplitude increased the capacity of the gelatin for scavenging free radicals, while the conformations that were adopted as a result of the treatments with 50% amplitude caused the free radical scavenger activity to decrease. These results could be attributed to the fact that, according to the results of the circular dichroism, the CD ratio of the random coil was the lowest in UPG-42 and UPG-52; however, more studies are needed to confirm this.

According to this assay, the gelatins in this study showed antioxidant activity in the range of 200–1000 $\mu\text{M TE/mg}$ of gelatin, and these results are comparable to hydrolysates of green beans (200–350 $\mu\text{M TE/mg sample}$) [28] and rainbow trout hydrolysates (400–1200 $\mu\text{M TE/g sample}$) [14].

3.8. Ferric Reducing Antioxidant Power

For FRAP, the UPG gelatins showed a significant increase in activity with respect to the CG. The highest activity was obtained for UPG-84 (732 $\mu\text{M TE}$) ($p < 0.05$), while the other UPGs showed lower activity (from 244 to 385 $\mu\text{M TE}$), and no significant difference was found between these gelatins ($p < 0.05$). This behavior might be attributed to the surface hydrophobicity and the random coil ratio of the gelatin.

According to these results, the UPGs in this study had ferric reducing antioxidant power in the range from 244 to 732 TE/mg of gelatin, and these results are lower than those obtained for horse gram hydrolysates (~1100 $\mu\text{M TE/mg sample}$) [27] but higher than those obtained for seabass collagen hydrolysates (~2–6 $\mu\text{M TE/g sample}$) [11]. Thus, the antioxidant activity of the UPG in this study is comparable to those obtained for gelatins that were subjected to chemical modifications due to the breaking of peptide bonds [11,27]; in contrast, this study was limited to the interruption of intramolecular interactions due to the effect of cavitation [29].

In general, from both antioxidant activity assays, it can be concluded that high-intensity ultrasound treatments improved the antioxidant properties of the gelatins by transferring an electron to stabilize the radicals. Further studies should be carried out for the antioxidant evaluation of the UPGs by hydrogen atom transfer to more comprehensively determine the antioxidant activity of these gelatins.

4. Conclusions

High-intensity ultrasonic pulse treatments that were applied to tilapia skin gelatin had beneficial effects on antioxidant activity, as a single electron transfer antioxidant to reduce oxidized intermediates, and in protein solubility. These improvements can be associated with changes in pH, surface hydrophobicity, and the ordered secondary structures (both the β -sheet and the α -helix) with no significant effect on the random coil and the primary structure of gelatin. The electrophoretic analysis confirmed that the treatments did not produce protein hydrolysis. As could be seen from the different

treatments used in this work, the ultrasound treatment with a frequency of 20 kHz and 100% amplitude for two minutes with an intensity of 84 W/cm² induced conformational changes in the tilapia skin gelatin that significantly improved its solubility and antioxidant properties. These findings could recommend the application of more HIU treatments of gelatin to improve other biological and functional activities. These studies can boost the use of green technologies to increase the potential of fishery waste as tilapia skin gelatin, with the advantages of a short time and economic process.

Author Contributions: Conceptualization, D.A.C.-A., S.R.-C., and J.L.A.-M.; Methodology, J.L.A.-M., R.G.V.-M., and W.T.-A.; Software, F.C.-C., and H.d.C.S.-O.; Formal analysis, D.A.C.-A., and F.C.-C.; Investigation, F.C.-C., S.C.-H., H.d.C.S.-O.; writing—original draft preparation, D.A.C.-A.; writing—review and editing, D.A.C.-A., J.L.A.-M., and W.T.-A.; Project administration and Supervision, S.R.-C. All authors have read and agreed to the published version of the manuscript.

Funding: This research received no external funding.

Acknowledgments: The authors acknowledge the support of CONACyT through postdoctoral grant.

Conflicts of Interest: The authors declare no conflict of interest.

References

1. Arzeni, C.; Martínez, K.; Zema, P.; Arias, A.; Pérez, O.E.; Pilosof, A.M.R. Comparative study of high intensity ultrasound effects on food proteins functionality. *J. Food Eng.* **2012**, *108*, 463–472. [[CrossRef](#)]
2. Song, K.M.; Jung, S.K.; Kim, Y.H.; Kim, Y.E.; Lee, N.H. Development of industrial ultrasound system for mass production of collagen and biochemical characteristics of extracted collagen. *Food Bioprod. Process.* **2018**, *110*, 96–103. [[CrossRef](#)]
3. Higuera-Barraza, O.A.; Del Toro-Sanchez, C.L.; Ruiz-Cruz, S.; Márquez-Ríos, E. Effects of high-energy ultrasound on the functional properties of proteins. *Ultrason. Sonochem.* **2016**, *31*, 558–562. [[CrossRef](#)] [[PubMed](#)]
4. Jambrak, A.R.; Mason, T.J.; Lelas, V.; Herceg, Z.; Herceg, I.L. Effect of ultrasound treatment on solubility and foaming properties of whey protein suspensions. *J. Food Eng.* **2008**, *86*, 281–287. [[CrossRef](#)]
5. Wang, J.Y.; Yang, Y.L.; Tang, X.Z.; Ni, W.X.; Zhou, L. Effects of pulsed ultrasound on rheological and structural properties of chicken myofibrillar protein. *Ultrason. Sonochem.* **2017**, *38*, 225–233. [[CrossRef](#)]
6. O'Sullivan, J.; Murray, B.; Flynn, C.; Norton, I. The effect of ultrasound treatment on the structural, physical and emulsifying properties of animal and vegetable proteins. *Food Hydrocoll.* **2016**, *53*, 141–154. [[CrossRef](#)]
7. Higuera-Barraza, O.A.; Torres-Arreola, W.; Ezquerro-Brauer, J.M.; Cinco-Moroyoqui, F.J.; Figueroa, J.R.; Marquez-Ríos, E. Effect of pulsed ultrasound on the physicochemical characteristics and emulsifying properties of squid (*Dosidicus gigas*) mantle proteins. *Ultrason. Sonochem.* **2017**, *38*, 829–834. [[CrossRef](#)] [[PubMed](#)]
8. Hu, H.; Wu, J.; Li-Chan, E.C.Y.; Zhu, L.; Zhang, F.; Xu, X.; Fan, G.; Wang, L.; Huang, X.; Pan, S. Effects of ultrasound on structural and physical properties of soy protein isolate (SPI) dispersions. *Food Hydrocoll.* **2013**, *30*, 647–655. [[CrossRef](#)]
9. Wu, D.; Wu, C.; Ma, W.; Wang, Z.; Yu, C.; Du, M. Effects of ultrasound treatment on the physicochemical and emulsifying properties of proteins from scallops (*Chlamys farreri*). *Food Hydrocoll.* **2019**, *89*, 707–714. [[CrossRef](#)]
10. Vera, A.; Valenzuela, M.A.; Yazdani-Pedram, M.; Tapia, C.; Abugoch, L. Conformational and physicochemical properties of quinoa proteins affected by different conditions of high-intensity ultrasound treatments. *Ultrason. Sonochem.* **2019**, *51*, 186–196. [[CrossRef](#)]
11. Chotphruethipong, L.; Aluko, R.E.; Benjakul, S. Hydrolyzed collagen from porcine lipase-defatted seabass skin: Antioxidant, fibroblast cell proliferation, and collagen production activities. *J. Food Biochem.* **2019**, *43*, e12825. [[CrossRef](#)] [[PubMed](#)]
12. Wu, Q.; Zhang, X.; Jia, J.; Kuang, C.; Yang, H. Effect of ultrasonic pretreatment on whey protein hydrolysis by alcalase: Thermodynamic parameters, physicochemical properties and bioactivities. *Process Biochem.* **2018**, *67*, 46–54. [[CrossRef](#)]

13. Ketnawa, S.; Martínez-Alvarez, O.; Benjakul, S.; Rawdkuen, S. Gelatin hydrolysates from farmed Giant catfish skin using alkaline proteases and its antioxidative function of simulated gastro-intestinal digestion. *Food Chem.* **2016**, *192*, 34–42. [[CrossRef](#)]
14. Nikoo, M.; Benjakul, S.; Yasemi, M.; Gavlighi, H.A.; Xu, X. Hydrolysates from rainbow trout (*Oncorhynchus mykiss*) processing by-product with different pretreatments: Antioxidant activity and their effect on lipid and protein oxidation of raw fish emulsion. *LWT-Food Sci. Technol.* **2019**, *108*, 120–128. [[CrossRef](#)]
15. Gutiérrez-Yurrita, P.J. La Acuicultura en México: II. Época actual y perspectivas. *Biol. Inf.* **2000**, *32*, 1–8.
16. Arpi, N.; Hardianti, E. Preparation and characterization of biodegradable film based on skin and bone fish gelatin. *IOP Conf. Ser. Earth Environ. Sci.* **2018**, *207*, 012050. [[CrossRef](#)]
17. Bradford, M.M. Rapid and sensitive method for quantitation of microgram quantities of protein utilizing principle of protein-dye binding. *Anal. Biochem.* **1976**, *72*, 248–254. [[CrossRef](#)]
18. Laemmli, U.K. Cleavage of structural proteins during the assembly of the head of bacteriophage T4. *Nature* **1970**, *227*, 680–685. [[CrossRef](#)]
19. Hayakawa, S.; Nakai, S. Relationships of hydrophobicity and net charge to the solubility of milk and soy proteins. *J. Food Sci.* **1985**, *50*, 486–491. [[CrossRef](#)]
20. Re, R.; Pellegrini, N.; Proteggente, A.; Pannala, A.; Yang, M.; Rice-Evans, C. Antioxidant activity applying an improved ABTS radical cation decolorization assay. *Free Radic. Biol. Med.* **1999**, *26*, 1231–1237. [[CrossRef](#)]
21. Benzie, I.F.; Strain, J.J. The ferric reducing ability of plasma (FRAP) as a measure of “antioxidant power”: The FRAP assay. *Anal. Biochem.* **1996**, *239*, 70–76. [[CrossRef](#)] [[PubMed](#)]
22. Shen, X.; Shao, S.; Guo, M. Ultrasound-induced changes in physical and functional properties of whey proteins. *Int. J. Food Sci. Tech.* **2017**, *52*, 381–388. [[CrossRef](#)]
23. Potaros, T.; Raksakulthai, N.; Runglerdkreangkrai, J.; Worawattanamateekul, W. Characteristics of collagen from Nile tilapia (*Oreochromis niloticus*) skin isolated by two different methods. *Nat. Sci.* **2009**, *43*, 584–593.
24. Kittiphattanabawon, P.; Sriket, C.; Kishimura, H.; Benjakul, S. Characteristics of acid and pepsin solubilized collagens from Nile tilapia (*Oreochromis niloticus*) scale. *Emir. J. Food Agric.* **2019**, *31*, 95–101. [[CrossRef](#)]
25. Chandrapala, J.; Zisu, B.; Palmer, M.; Kentish, S.; Ashokkumar, M. Effects of ultrasound on the thermal and structural characteristics of proteins in reconstituted whey protein concentrate. *Ultrason. Sonochem.* **2011**, *18*, 951–957. [[CrossRef](#)] [[PubMed](#)]
26. Muyonga, J.H.; Cole, C.G.B.; Duodu, K.G. Fourier transform infrared (FTIR) spectroscopic study of acid soluble collagen and gelatin from skins and bones of young and adult Nile perch (*Lates niloticus*). *Food Chem.* **2004**, *86*, 325–332. [[CrossRef](#)]
27. Kittiphattanabawon, P.; Benjakul, S.; Sinthusamran, S.; Kishimura, H. Gelatin from clown featherback skin: Extraction conditions. *LWT-Food Sci. Tech.* **2016**, *66*, 186–192. [[CrossRef](#)]
28. Bhaskar, B.; Ananthanarayan, L.; Jamdar, S.N. Effect of enzymatic hydrolysis on the functional, antioxidant, and angiotensin I-converting enzyme (ACE) inhibitory properties of whole horse gram flour. *Food Sci. Biotechnol.* **2019**, *28*, 43–52. [[CrossRef](#)]
29. Ozuna, C.; Paniagua-Martínez, I.; Castaño-Tostado, E.; Ozimek, L.; Amaya-Llano, S.L. Innovative applications of high-intensity ultrasound in the development of functional food ingredients: Production of protein hydrolysates and bioactive peptides. *Food Res. Int.* **2015**, *77*, 685–696. [[CrossRef](#)]

